

Review: Two- and three-dimensional growth modes of nitride layers

K. Pakula^{*1}, J. M. Baranowski¹, and J. Borysiuk²

¹ Institute of Experimental Physics Warsaw University, Hoża 69, 00-681 Warsaw, Poland

² Institute of Electronic Materials Technology, Wólczyńska 133, 01-919 Warsaw, Poland

Received 21 May 2007, accepted 10 September 2007

Published online 10 November 2007

Key words MOVPE, nitride, dislocations.

PACS 68.55.-a, 61.72.Ff

Heteroepitaxial three dimensional (3D) and two dimensional (2D) growth modes of nitride layers on sapphire substrates are discussed. It is shown that the 3D or 2D growth mode of AlGaIn layers depends predominantly on the growth conditions of the underneath low temperature (LT) nucleation layer. Commonly described in literature 3D growth mode is achieved on LT GaN or AlN nucleation layer grown relatively fast. Successive growth of secondary layer at high temperature begins from separated sites, where individual 3D crystallites are formed. Threading dislocations present in crystallites bend on their facets, which reduces the quantity of dislocations. However, slight crystallographic misorientations between crystallites lead to the creation of new dislocations during coalescence of the crystallites. As a result, edge and mix dislocations appear at similar densities of about 10^9 cm^{-2} . Modification of growth conditions of LT AlN nucleation layer, especially reduction of their growth rate, leads to drastic changes in properties of the layer. Successive growth of secondary AlGaIn layer at high temperature starts evenly on whole surface retaining atomic flatness. Thus growth at high temperature occurs only by 2D mode. Therefore, it is possible to grow a very thin AlGaIn layers directly on top of LT nucleation layer. Such layers contain large number (10^{10} cm^{-2}) of edge dislocations, and relatively small number (less than 10^8 cm^{-2}) of mix dislocations. It is also shown that the decisive factor determining the growth mode of AlN nucleation layer is a growth of the first few atomic layers on substrate surface. The slow growth of these few first atomic layers decide about the 2D growth mode, and the fast one about the 3D one. The model explaining this difference is presented as well.

© 2007 WILEY-VCH Verlag GmbH & Co. KGaA, Weinheim

1 Introduction

Growth of nitride epitaxial layers has been in recent years intensively studied due to their application in short-wavelength optoelectronic and to the low crystalline quality of the material. One of the main problems connected with epitaxial growth of nitrides is lack of commercially available large size native substrates. Sapphire or 6H-SiC substrates are typically used for nitride based applications. These substrates, however, are poorly matched to nitride layers. There is, for example, a lattice mismatch of 16% and 13% between *c*-plane sapphire substrates and GaN and AlN lattice constants, respectively. As a result, growth of nitride layers on such substrates lead to the formation of three-dimensional (3D) crystallites [1,2]. These crystallites are slightly twisted and tilted with respect to the *c*-axis of sapphire substrate. Further growth leads to island formation followed by their coalescence. This coalescence process generates additional threading dislocations. Generally, threading dislocations are formed to reduce the biaxial compressive strains [3,4], resulting from the lattice mismatch between the lattice constants of the layer and the substrate. The other reason of generation of dislocations is the mismatch in the thermal expansion coefficients of the layer and the substrate during the post-growth cooling.

* Corresponding author: e-mail: krzysztof.pakula@fuw.edu.pl

Many studies indicate that threading dislocations are electrically active. Theoretical calculations predict that either dislocations themselves [5-8] or electrically active point defects and impurities accumulated at dislocations due to existing stress fields [9,10], introduce electronic states in the energy gap. Therefore, it has been predicted that dislocations may act as non-radiative recombination centers [8]. Electrical activity of dislocations has also been confirmed experimentally [11-13].

Crystalline perfection of epitaxial structures is a major factor that influences practical applications of nitrides. Comprehension of the epitaxial growth mechanisms and crystalline defect generation is very important for further improvement of epitaxial structures. Understanding of the epitaxial growth process is important especially for III-V nitride heterostructures, not only due to the lack of lattice-matched substrates but also due to a high lattice mismatch between different nitride compounds. Crystalline defects originate from point defects at the growing surface due to the local strain related to lattice mismatch at the growth temperature. Point defects appear on the growth surface at the moment of coalescence of nucleus [14,15]. Diffusion of point defects and their structural transformations lead to the creation of clusters of point defects, stacking faults, dislocations and dislocations accumulation. The high density of crystalline defects in nitride epitaxial structures has a significant influence on device applications, and still is a major technological challenge [16-18]. In spite of a number of studies addressed to crystalline perfection and defect generation in initial stages of epitaxial growth [19] and in thicker layers [20], these phenomena are still not completely understood.

It is known that the LT nucleation layer is required for the heteroepitaxial growth of nitride layers. Optimization of the nucleation layers appears to be the focus of many investigations [1,21-24]. Conventional way of LT nucleation layer growth and its recrystallization at high temperature, provides well separated nucleation sites, and thus stimulates the 3D growth mode of the successive nitride layer [25]. Transition to the 2D growth mode takes place after individual crystalline islands coalesce together. This finally leads to a smooth layer which grows in the 2D mode. Thus, the transition from 3D to 2D growth mode takes place after growth of a few hundreds of nm thick GaN layer.

In this paper we discuss the influence of the growth conditions of low temperature nucleation layer of GaN and AlN on the structural properties of the GaN and AlGaN epitaxial layer.

2 Experimental

Epitaxial processes were performed in MOVPE system with horizontal reactor, using hydrogen as a carrier gas. Trimethylgallium (TMGa), trimethylaluminum (TMAI) and ammonia (NH₃) were used as precursors, and sapphire as substrates. The low temperature (LT) GaN and AlN nucleation layers were grown at temperatures ranging from 400 to 700°C at total pressure between 50 and 400 mbar. Growth temperature of secondary GaN or AlGaN layers was changed between 900 and 1100°C, and total pressure between 100 and 400 mbar.

The observation of the microstructure of LT nucleation layers was made by Atomic Force Microscopy (AFM). The determination of density of dislocations was done by the AFM method as well. Transmission Electron Microscopy (TEM) was used to study microstructure of thick layers. Cross-sectional TEM specimens were prepared by the standard method of mechanical pre-thinning followed by Ar ion milling. The contrast and high resolution TEM observations were made on JEOL JEM 3010 microscope operating at 300 kV. The two-beam analysis was employed to determine the Burgers vectors of dislocations.

3 Experimental results

Growth of GaN on LT GaN nucleation layer Each epitaxial process was started from annealing of sapphire substrate at 1100°C in hydrogen atmosphere. Next, temperature was decreased to 400-800°C and growth of nucleation layer was started. To avoid metal droplets formation, ammonia flow was opened 10 seconds before TMGa flow. The time of growth and the reagents flow rates were matched to obtain 30 nm thick layer.

Typical AFM image of the LT GaN nucleation layer surface is shown in figure 1. The layer is continuous and homogeneous, with roughness below 10 nm. It probably consists of large quantity of grains with size between 20 and 40 nm. This image does not change significantly in wide range of growth parameters or due to annealing process. Therefore, it is more instructive to study the properties of LT nucleation layers by

observation of their influence on secondary layers, grown on their top at high temperature. The LT growth of GaN is governed mostly by direct chemical reaction between ammonia and TMGa with substrate surface acting as a catalyst. Thus, it could be expected that the temperature is the most influential parameter of the growth.

After the completing of growth of LT nucleation layer, the temperature was increased to 900–1100°C. Any additional annealing stage or recrystallisation process did not influence the growth in a significant way. Thus, the growth of all described layers started immediately after reaching the destined temperature.

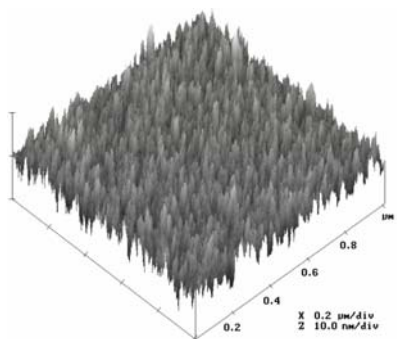


Fig. 1 AFM image of LT GaN nucleation layer of average thickness 30 nm grown at sapphire substrate at 500°C.

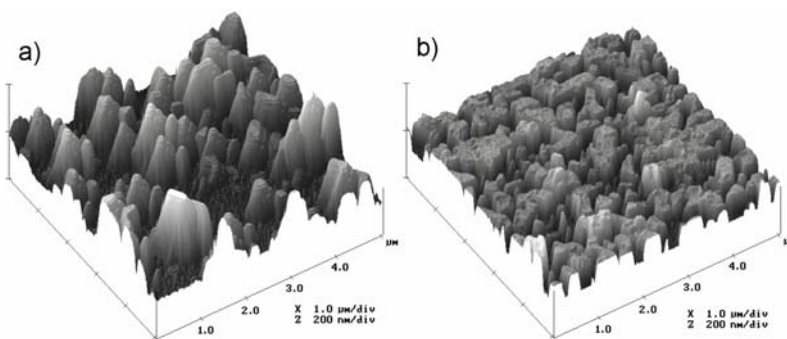


Fig. 2 AFM images of GaN grown at 1100°C for 60 s on LT GaN nucleation layer obtained at (a) 500°C and (b) 700°C.

Figure 2a and b show the AFM images of the GaN grown at 1100°C for 60 s on LT GaN nucleation layers obtained at different temperatures. The expected growth rate for flat layer grown at these conditions was about 2500 nm/h. Thus, after 60 seconds the flat layer with thickness of 40 nm should be obtained. It is seen that secondary nucleation takes place at distinctly separated sites with a density of about $1 \mu\text{m}^{-2}$. Each nucleation seed grew extremely fast as 3D crystallite reaching up to 200 nm heights. It is still visible LT nucleation layer between the crystallites. The Efficiency of growth rate seems to be unchanged. With increasing the growth temperature of LT nucleation layer, secondary nucleation becomes denser and, consequently crystallites are shorter. It seems that the time needed for the coalescence of crystallites became shorter, but above 700°C a qualitative change takes place.

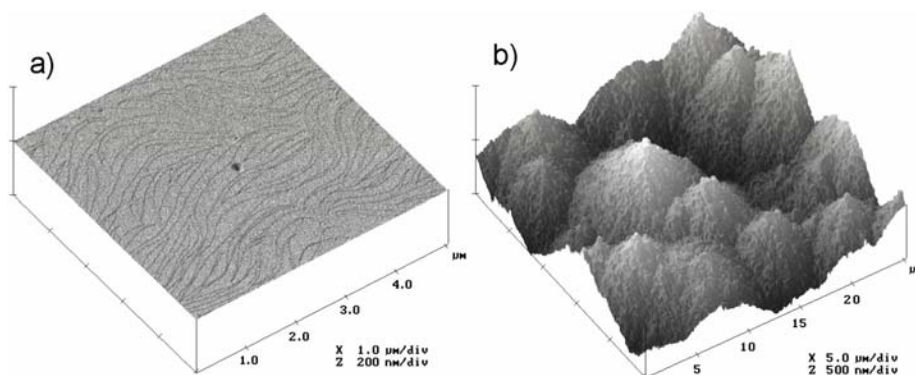


Fig. 3 AFM images of GaN grown at 1100°C for 3600 s on LT GaN nucleation layer obtained at (a) 700°C and (b) 800°C.

Figure 3a and b show the AFM images of GaN layers grown at the same conditions for 3600 s on LT GaN nucleation layers obtained at 700 and 800°C, respectively. The first image is typical for properly grown GaN layers with Ga-polarity. The second image shows the surface with large hills with height reaching 1000 nm. It is typical for GaN with N-polarity. This dramatic change results probably from interaction between ammonia and sapphire surface starting at higher temperature.

The influence of the growth temperature on the secondary GaN layer was also investigated. The optimal growth temperature of the nucleation layer of 500°C was chosen and the secondary layer was grown at 900–1100°C for 60 s. The AFM image of morphology of such grown GaN is shown in figures 2a and 4.

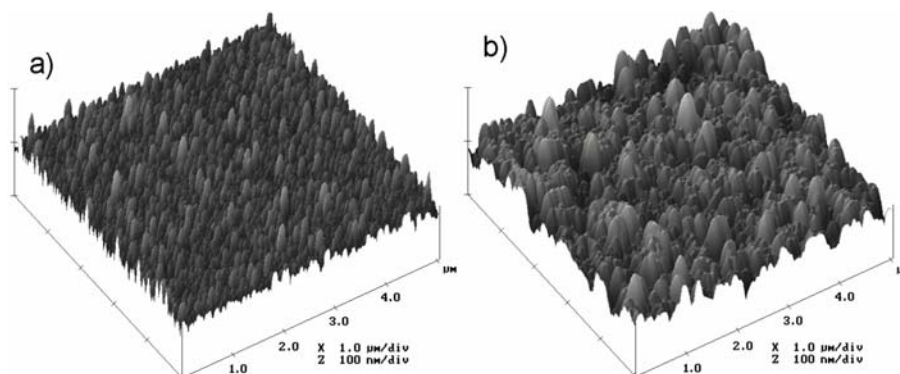


Fig. 4 AFM images of GaN grown at (a) 900 and (b) 1000°C for 60 s on LT GaN (30nm) obtained at 500°C. Note different vertical scale here in comparison with that in figure 2

It may be seen that lower temperature enables much denser secondary nucleation. However, even prolonged growth under these conditions does not lead to a smooth layer. The surface stays covered with crystallites and a transition to the 2D growth does not take place. On the other hand, increase of the growth temperature of the secondary layer leads to larger sizes of individual crystallites and delays their coalescence.

In conclusion, it was found that the growth of GaN epilayers is in full agreement with the ideas proposed by Hiramatsu et al. [26]. The LT GaN nucleation layer provides good source of nucleating sites for individual crystallites, which are grown at high temperature. These individual crystallites form islands which subsequently coalesce together. Finally, after reaching a thickness of about 200–500 nm, the smooth layer is formed and the growth mode changes from the 3D to the 2D one.

Growth of AlGaIn on LT AlN nucleation layer The influence of LT AlN nucleation layer on the mode of growth of AlGaIn was investigated. It is known that AlN growth rate strongly depends on total pressure in the reactor. To achieve better growth efficiency, lower pressure is required [24]. Therefore, LT AlN nucleation layer is usually grown at low pressure in the MOVPE reactor.

Two types of LT AlN nucleation layer were grown. The first one was more conventional; the total pressure was 50 mbar and the growth time was 100 s. The final thickness of the nucleation layer was about 30 nm. The second type was grown at 400 mbar. To obtain 30 nm thickness of such a layer, it was necessary to increase the TMAI flow to three times and the growth time by a factor of 10. The growth temperature was in both cases equal to 650°C.

The growth of secondary AlGaIn layer was made at 1100°C and the total pressure at the reactor was 200 mbar. Figure 5a and b shows AFM images of the AlGaIn (10% of Al content) layers after 60 s of growth.

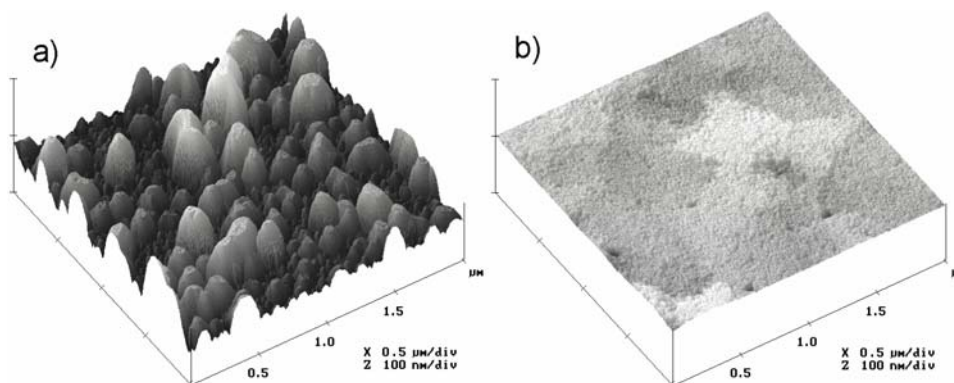


Fig. 5 AFM images of AlGaIn layers grown at 1100°C for 60 s on LT AlN nucleation layer obtained at (a) fast and (b) slow growth.

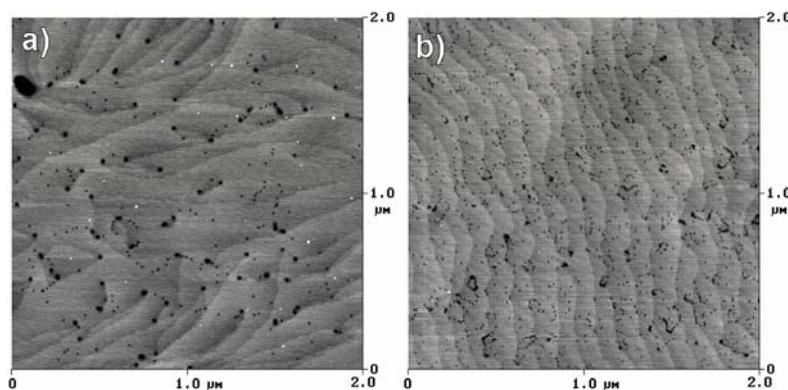


Fig. 6 AFM images of AlGaIn layers grown at 1100°C for 3600 s on LT AlN nucleation layer obtained at (a) fast and (b) slow growth.

In the case of LT AlN nucleation layers obtained by using fast growth, the results are similar to those observed for the GaN layer on LT GaN nucleation layers. Secondary nucleation centers are created at several separated locations, leading to the growth of independent 3D crystallites. Further growth leads to increase of their size and to coalescence, as in the case of GaN.

Figure 6a shows AFM image of about 2 μm thick AlGaIn layer grown in the same way, but for 3600 s. The surface of the sample is flat with a high density of threading dislocations manifested as small holes. Larger holes are connected with mixed dislocations with screw component and atomic steps are originating in these sites. Smaller holes are connected with edge dislocations, which do not disturb the shape of atomic steps. The total density of dislocations approaches 10^{10} cm^{-2} . Both types of dislocations appear with comparable densities.

The growth of LT AlN nucleation layer at 400 mbar pressure (slow growth) gives different results. After 60 s of growth the secondary AlGaIn layer covers the whole surface (see Fig. 5b). The roughness of this surface does not exceed 10 nm. The expected average thickness of the layer is about 40 nm. This suggests that growth of the secondary layer takes place on the whole surface, immediately after the growth starts at high temperature. These layers grow in the 2D mode.

Figure 6b shows the surface of the secondary layer grown in the same way, but for 3600 s. Surface is flat with atomic steps running without obstacles through several micrometers. This means that mixed dislocations do not appear on the observed area. More accurate measurement indicates that mixed dislocation density is below 10^8 cm^{-2} . At the same time the number of edge dislocations increases well above 10^{10} cm^{-2} level.

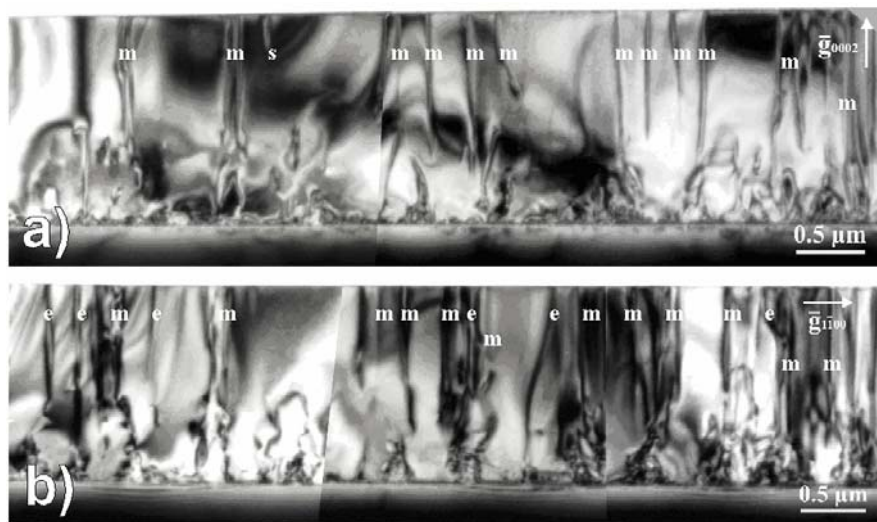


Fig. 7 Two-beam TEM images from the same area of AlGaIn layer grown in 3D mode: (a) bright field cross-section, $g = 0002$, screw and mixed dislocations in contrast; (b) bright field cross-section, $g = 1100$, edge and mixed dislocations in contrast; (m) mixed, (s) screw, (e) edge dislocations.

TEM study of 3D and 2D growth of AlGaN TEM measurements were carried out to clarify the mechanism connected with 3D and 2D growth mode of AlGaN layers. Low-magnification bright-field TEM micrographs of thick AlGaN sample grown in the 3D mode are shown in figure 7. A large number of dislocations is characteristic for nitride growth. In order to distinguish between different types of dislocations these micrograph were recorded for g-vector parallel to [0002] direction (Fig. 7a) and to [1-100] direction (Fig. 7b). It is seen that three kinds of dislocations are present: mixed ones with Burgers vector $b = 1/3\langle 11-23 \rangle$, screw ones with $b = [0001]$ and edge ones $b = 1/3\langle 11-20 \rangle$. The densities were estimated at $2.1 \cdot 10^9 \text{ cm}^{-2}$, $1.3 \cdot 10^8 \text{ cm}^{-2}$ and $7.5 \cdot 10^8 \text{ cm}^{-2}$ for the mixed, screw and edge type dislocations respectively. The dominant dislocations are mixed type, with a screw component, and they control the step formation on the surface.

A high-resolution TEM micrograph of the AlGaN/AlN interface for the fast grown LT AlN is shown in figure 8. The trapezoid crystallites are seen, as described by Hiramatsu et al. [26]. The stacking faults are generated on the grain boundaries of trapezoid crystallites. It is interesting to note that stacking faults bend dislocations, as indicated in figure 8. This is one of the reasons for lower density of threading dislocations, present in layers grown in the 3D growth mode. The other important factor is that threading dislocations bend on the facets of individual crystallites. Bending of threading dislocations on facets of crystallites has recently been demonstrated to reduce the density of dislocations by in situ silane treating the surface of GaN during their growth at high temperature [27].

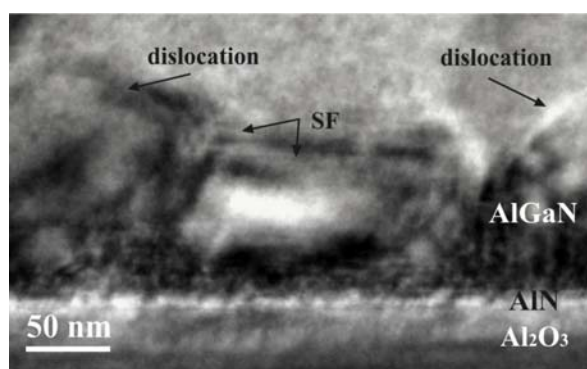


Fig. 8 Cross-section TEM micrograph of AlN/AlGaN interface region. SF denotes stacking faults, interacting with dislocations.

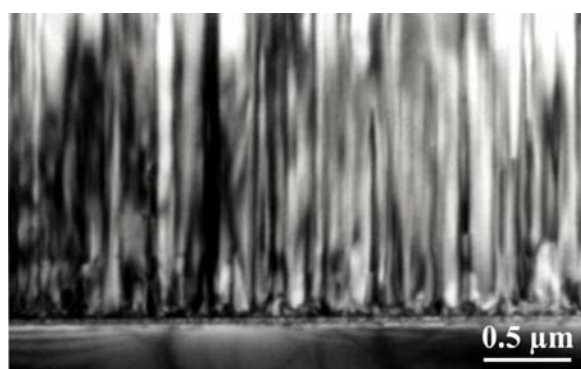
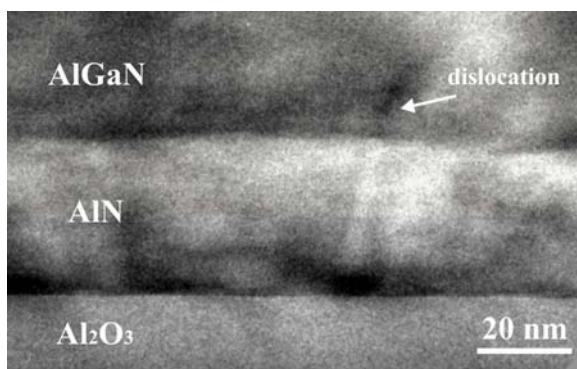


Fig. 9 Cross-section TEM image ($g = 1\bar{1}00$) of AlGaN layer grown in 2D mode with high density of edge dislocations.

Fig. 10 Cross-section TEM image of AlN/AlGaN interface, demonstrating the creation of dislocations on coalescence of island. The interface is remarkably flat.



A low-magnification bright-field TEM micrograph of thick AlGaN sample grown in the 2D mode (on slowly grown LT AlN) is shown in figure 9. It is seen that the density of dislocation is enormous. The density of dislocations found by AFM method in this layer about $3 \cdot 10^{10} \text{ cm}^{-2}$, almost one order of magnitude higher than in the case of the 3D growth mode. However, the TEM results indicate that they are predominantly edge dislocations. The high resolution TEM micrograph of the slowly grown AlGaN/AlN interface is shown in figure 10. It is seen that edge dislocations originate in the LT nucleation layer.

The differences between the 3D and 2D growth mode were demonstrated by using growth of AlGaN with oscillating amount of Al. The growth of AlGaN can often be performed in such conditions that amount of Al

incorporated in grown layer has oscillatory character [28]. The TEM micrograph, showing the AlGa_N layer grown in 3D mode and in such conditions that superlattice of Al content is formed, is shown in figure 11a. The oscillatory character of Al reveals the 3D growth in the initial stage of growth of the layer. This micrograph also reveals that threading dislocations are formed at island boundaries. This picture confirms our knowledge about the conventional way of growth of nitrides.

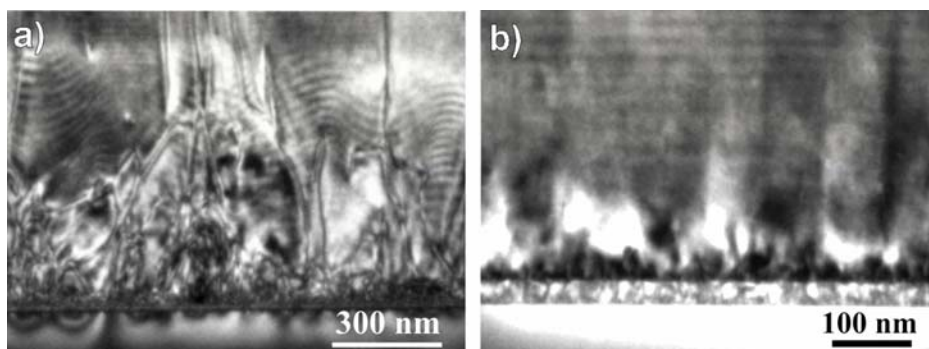


Fig. 11 TEM images of AlGa_N layer with oscillating Al content, grown in (a) 3D mode and (b) 2D mode. The shape of the free surface during growth with large height differences is visible in (a), and flat in (b).

The same method of growth has been used for the AlGa_N layer obtained on slowly grown LT AlN nucleation layer. TEM micrograph of this layer is shown in figure 11b. The oscillations of Al content start directly over LT nucleation layer, and are parallel to the substrate in whole volume of the layer. They directly show that the growth is indeed in the 2D mode.

4 Discussion

The investigations presented here reveal basic differences between LT GaN and LT AlN nucleation layers. The growth of LT GaN nucleation layer always leads to the formation of 3D crystallites in the successively grown layer. These crystallites are tilted and twisted with respect to each other. The tilt of crystallites is responsible for the formation of mixed and screw dislocations, which are often generated at their boundaries. Thus, the growth of GaN layer is always connected with the presence of a zone where crystallites grow to islands. When individual islands coalesce together, stacking faults are generated in addition to dislocations. After reaching the stage of full coalescence of islands, 2D growth takes place. Thus, 2D growth takes place after the formation of a relatively thick GaN layer of about 500 nm. Another condition for the 2D growth is a relatively high temperature of about 1050°C of the main layer growth.

The situation is different in the case of LT AlN nucleation layer. The LT AlN nucleation layer opens two possible ways for the AlGa_N growth modes. The nucleation layer grown at low pressure gives relatively high growth, and this stimulates the 3D growth. This mode is similar to that observed for the growth on the LT GaN nucleation layer. However, the other growth mode is observed when the LT AlN nucleation layer is grown slowly, which takes place at relatively high pressure. In this case, the 2D growth mode of AlGa_N is observed directly on the LT AlN nucleation layer. Apparently, the slow growth of the AlN nucleation layer creates such a large density of nucleation sites that secondary layer growth starts in the 2D fashion. Edge dislocations are generated during the 2D growth, indicating that individual crystallites in the LT AlN nucleation layer are predominantly twisted around the c-axis with respect to each other. Twisting of crystallites introduces edge dislocations on the boundaries between them. The high edge dislocation density, of the order $3 \cdot 10^{10} \text{ cm}^{-2}$ in AlGa_N layer grown in the 2D mode, indicates that individual crystallites are indeed small and are mainly misoriented by twist around the c-axis.

In contrast to the above 2D mode, layers grown in the 3D mode have incorporated mechanisms of dislocation elimination. Threading dislocations bend on facets of individual crystallites, which in this growth mode are twisted relative to the c-axis. Also, the presence of stacking faults above coalescing islands creates another way of bending dislocations. There is probably an additional mechanism of reducing strain in the 3D growth mode. As seen in figure 11a, sapphire underneath LT nucleation layer is deteriorated. This observation

was reported previously [29]. The formation of subgrain boundaries in the AlN nucleation layer is observed above the sites of deterioration of sapphire. These deteriorations were associated with oxygen outdiffusion from sapphire [30]. However, these deteriorations are present only in the case of the AlN nucleation layers grown in the 3D mode. They are not observed when the AlN nucleation layer is grown with a slow rate, in the 2D mode, in spite of that both 2D and 3D growths occur at the same temperature. Therefore, it seems that the deterioration is caused by the generation of defects into sapphire substrate, which relieve some of the strain accumulated inside of individual crystallites, which stimulate the 3D growth mode.

The question arises why slow or fast growth of AlN nucleation layer leads to so different growth modes of the successive AlGaIn layer. To throw some light on this problem, the following experiment was performed. The AlN nucleation layer growth was started at 400 mbar pressure corresponding to growth in the slow mode. After deposition of about 3 nm of the layer, the pressure was reduced to 50 mbar, and the remaining 20 nm of AlN was grown faster. After that, the secondary AlGaIn layer was grown. It was found that the layer grows in the 2D mode. This indicates that the first few atomic layers of the AlN nucleation layer are decisive for the choice of the growth mode. Therefore, one can propose the following model of the growth. The slow growth of the AlN nucleation layer gives, in the first few seconds of growth, a very thin layer of AlN. Due to lattice mismatch between sapphire and AlN, relaxation of the strain is released predominantly by twisting individual grains around the c-axis. This leads to the generation of edge dislocations and this is the main mechanism of strain relaxation. This establishes a pattern of future 2D growth mode. Later, growth of the AlN nucleation layer and successive AlGaIn layer continues by the 2D mode.

It should be noted that the fast growth of the AlN nucleation layer allows for local fluctuations of the thickness and local formation of 3D crystallites, which relieve strain via tilt of the c-axis with respect to the c-axis of sapphire. This establishes a pattern appropriate for the 3D mode of growth of the successive layer.

In conclusion, there are two modes of growth of AlGaIn on the AlN nucleation layer. The slow growth of the first atomic layers of AlN allows establishing 2D growth. AlGaIn grows in this case layer by layer, and it is possible to obtain smooth and very thin samples of the order of 50 nm. However, this is at expense of a high density of edge dislocation of the order $3 \cdot 10^{10} \text{ cm}^{-2}$. The fast growth of AlN nucleation layer leads to the 3D growth. To achieve transition to the 2D growth mode in this case, one needs to get relatively thick samples of the order of 1000 nm. Advantage of the 3D growth mode is relatively low density of dislocations, which are predominantly of mixed type. In contrast to this, the advantage of the 2D growth is that one gets layer with dislocations predominantly of the edge type. One may expect that they are not so harmful to the performance of devices as are the mixed and screw ones.

References

- [1] H. Amano, N. Sawaki, I. Akasaki, and Y. Toyoda, *Appl. Phys. Lett.* **48**, 353 (1986).
- [2] S. Nakamura, *Jpn. J. Appl. Phys.* **30**, L1705 (1991).
- [3] H. Amano, K. Hiramatsu, and I. Akasaki, *Jpn. J. Appl. Phys.* **27**, L1384 (1988).
- [4] T. Detchprohm, K. Hiramatsu, K. Itoh, and I. Akasaki, *Jpn. J. Appl. Phys.* **31**, L1454 (1992).
- [5] A. F. Wright and U. Grossner, *Appl. Phys. Lett.* **73**, 2751 (1998).
- [6] K. Leung, A. F. Wright, and E. B. Stechel, *Appl. Phys. Lett.* **74**, 2495 (1999).
- [7] S. M. Lee, M. A. Belkhir, X. Y. Zhu, Y. H. Lee, Y. G. Hwang, and T. Frauenheim, *Phys. Rev. B* **61**, 16033 (2000).
- [8] J. E. Northrup, *Appl. Phys. Lett.* **73**, 2288 (2001).
- [9] J. Elsner, R. Jones, P. K. Stich, V. D. Porezag, M. Elstner, T. Frauenheim, M. I. Heggie, S. Oberg, and P. R. Briddon, *Phys. Rev. Lett.* **79**, 3672 (1997).
- [10] J. Elsner, R. Jones, M. I. Heggie, P. K. Stich, T. Frauenheim, S. Oberg, and P. R. Briddon, *Phys. Rev. B* **58**, 12571 (1998).
- [11] P. J. Hansen, Y. E. Stausser, A. N. Ericson, E. J. Tarsa, P. Kozodoy, E. G. Brazel, J. P. Ibbetson, U. Mishra, V. Narayanamuturi, S. P. DenBaars, and J. S. Speck, *Appl. Phys. Lett.* **72**, 2247 (1998).
- [12] D. Cherns and C. G. Jiao, *Phys. Rev. Lett.* **87**, 8720 (2001).
- [13] J. W. P. Hsu, H. M. Ng, A. M. Sergent, and S. N. G. Chu, *Appl. Phys. Lett.* **81**, 3579 (2002).
- [14] L. E. Shako, D. J. Srolovitz, and J. Tersoff, *Phys. Rev. B* **62**, 8397 (2000).
- [15] A. A. Chernov, *Modern Crystallography III, Crystal Growth*, Springer, Berlin, Heidelberg, New York, Tokyo, 1984 (Chapters 1, 2).
- [16] H. Morkoc, S. Strite, G. B. Gao, M. E. Lin, B. Sverdlov, and M. Burns, *J. Appl. Phys.* **76**, 1363 (1994).
- [17] S. C. Jain, M. Willander, J. Narayan, and R. Van Overstraeten, *J. Appl. Phys.* **87**, 965 (2000).
- [18] S. J. Pearton, J. C. Zolper, R. J. Shul, and F. Ren, *J. Appl. Phys.* **86**, 1 (1999).

- [19] F. A. Ponce, B. S. Krusor, J. S. Major Jr., W. E. Plano, and D. F. Welch, *Appl. Phys. Lett.* **67**, 410 (1995).
- [20] V. Darakchieva, J. Birch, M. Schubert, T. Paskova, S. Tungasmita, G. Wagner, A. Kasic, and B. Monemar, *Phys. Rev. B* **70**, 045411 (2004).
- [21] X. H. Wu, D. Kapolnek, E. J. Tarsa, B. Heyning, S. Keller, B. P. Keller, U. Mishra, S. P. DenBaars, and J. S. Speck, *Appl. Phys. Lett.* **68**, 1371 (1996).
- [22] X. H. Wu, L. M. Brown, D. Kapolnek, and S. Keller, *J. Appl. Phys.* **80**, 3228 (1996).
- [23] S. Nakamura, *Jpn. J. Appl. Phys.* **30**, L1705 (1991).
- [24] L. Sugiura, K. Itaya, J. Nishino, H. Fujimoto, and Y. Kokubun, *J. Appl. Phys.* **82**, 498 (1997).
- [25] H. Marchand, L. Zhao, N. Zhang, B. Moran, R. Coffie, U. K. Mishra, J. S. Speck, S. P. DenBaars, and J. A. Freitas, *J. Appl. Phys.* **89**, 7846(2001).
- [26] K. Hiramatsu, S. Itoh, H. Ammano, I. Akasaki, N. Kuwano, T. Shiraishi, and K. Oki, *J. Cryst. Growth* **115**, 628 (1991).
- [27] K. Pakuła, R. Bożek, J. M. Baranowski, J. Jasinski, and Z. Liliental-Weber, *J. Cryst. Growth* **267**, 1 (2004).
- [28] K. Pakuła, J. Borysiuk, R. Bożek, and J. M. Baranowski, *J. Cryst. Growth* **296**, 191 (2006).
- [29] S. Ruvimov, Z. Liliental-Weber, J. Washburn, H. Ammano, I. Akasaki, and H. Koike, *Mater. Res. Soc. Symp. Proc.* **423**, 487 (1996).
- [30] S. Ruvimov, *III-V Nitride Semiconductors: Defects and Structural Properties*, ed. M. O. Manashreh, Elsevier Science BV, p. 52 (2000).